A Journal of the Gesellschaft Deutscher Chemiker

Angewandte International Edition

GDCh

Chemie

www.angewandte.org

Accepted Article

Title: Morphology Reserved Synthesis of Discrete Nanosheets of CuO@SAPO-34 and Pore Mouth Catalysis for One-pot Oxidation of Cyclohexane

Authors: Weiping Ding, Xiangke Guo, Mengxia Xu, Minyi She, Yan Zhu, Taotao Shi, Zhaoxu Chen, Luming Peng, Xuefeng Guo, and Ming Lin

To be cited as: *Angew. Chem. Int. Ed.* 10.1002/anie.201911749
Angew. Chem. 10.1002/ange.201911749

Link to VoR: http://dx.doi.org/10.1002/anie.201911749
http://dx.doi.org/10.1002/ange.201911749

WILEY-VCH

10.1002/anie.201911749

WILEY-VCH

Morphology Reserved Synthesis of Discrete Nanosheets of CuO@SAPO-34 and Pore Mouth Catalysis for One-pot Oxidation of Cyclohexane

Xiangke Guo,[a] Mengxia Xu,[a] Minyi She,[a] Yan Zhu,[a] Taotao Shi,[a] Zhaoxu Chen,[a] Luming Peng,[a] Xuefeng Guo,*[a] Ming Lin,*[b] and Weiping Ding*[a]

Dedicated to the 100th anniversary of the School of Chemistry and Chemical Engineering, Nanjing University

Abstract: Discrete nanosheets of silicon-doped $AlPO_4$ molecular sieves (SAPO-34) in thickness of ~7 nm have been prepared following a mechanism of morphology reserved synthesis with a lamellar aluminum phosphate as the precursor. Some cages of the nanosheets are *in-situ* incorporated with copper oxide clusters during the preparation. The CuO@SAPO-34 nanosheets have huge external surface with large numbers of (010) channel pores showing up on the surface and, on average, the copper oxide clusters occupy the outmost cages in a possibility larger than 50% due to the super thin morphology. The distinctive configuration introduces a new concept of pore mouth catalysis for practical reactions, i.e., a reactant molecule in a size larger than the pores cannot enter the interior of molecular sieves but a part of it can interact with the copper oxide clusters through the pore. As a heterogeneous catalyst, the CuO@SAPO-34 nanosheet has shown the top catalytic performance up to date, for one-pot oxidation of cyclohexane by O_2 to adipic acid, a key compound for the manufacture of nylon-66 produced in industry so far only using a non-green method of nitric acid oxidation.

The reactive nanoclusters enclosed in and tuned by surrounded regular porous materials have been paid much research attention recently, thanks to their excellent performances for certain catalytic reactions.[1] For such catalysts, the surrounding materials confine and tune the reactive centers in many aspects and bring synergistic activities and shape/size selectivities.[2] The bulk 3D zeolitic framework limits the access of large molecules to the internal active centers which may locate deeply in the molecular sieves and also cannot be contacted by reactant through channel pores.[3] It is a great interest to create a kind of novel catalytic material which consists of ultrathin and well-crystallized molecular sieves with larger external surface and numerous exposed pores. The reactive centers, e.g., heteroclusters confined in the zeolitic cages and/or the zeolitic acidic sites, are limited by the zeolitic framework but easily accessed by a part of a reactant molecule through the pores, though the reactive molecule cannot enter the interior of the molecular sieves as a whole, due to the super thin structure.[4] The particular configuration should be capable of offering unpredictable catalytic performances. [5]

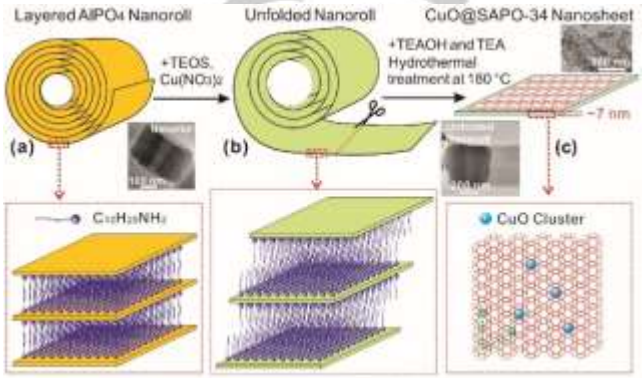

Figure 1. Schematic show of the formation process of CuO@SAPO-34 nanosheets. (a) Layered alumina phosphate nanoroll precusor with $C_{12}H_{25}NH_2$ in between the layers; (b) Unfolded nanoroll induced by the insertion of TEOS and $Cu(NO_3)_2$; (c) CuO@SAPO-34 nanosheets formed after hydrothermal treatment in presence of tetraethylamonium hydroxide (TEAOH) and triethylamine (TEA).

There have been two important breakthroughs on the synthesis of super thin molecular sieves respectively reported by Ryoo *et al* (2009) and Tsapatsis *et al* (2017), which are extremely noticeable to scientific community.[4b,5] And recently a novel assembly–disassembly–organisation–reassembly (ADOR) method has been used for the synthesis of 2D zeolites.[5d] Moreover, it is an extreme challenge to synthesize non-layered molecular sieves with 2D ultrathin structure for chemists of molecular sieves and materials because the process of molecular sieves crystallization and growth is controlled thermodynamically and 2D ultrathin structure is very unstable in nature due to the high surface energy.[4b]

Herein, we report a novel topoinvariant synthesis of discrete nanosheets of CuO@SAPO-34 by an *in-situ* transformation and re-crystallization of a well-defined super thin aluminum phosphate. During the preparation, the silicon doping to the zeolitic framework and the enclosure of CuO clusters in zeolitic cages can be introduced at the same time. The CuO@SAPO-34 nanosheets have huge external surface with large numbers of (010) channel pores showing upon the surface and the copper oxide clusters can be found at the outmost cages in a possibility large than 50% due to the super thin morphology, and on average, there are about 1/20 outmost pores can be found to contain a copper oxide cluster. The sample of CuO@SAPO-34 nanosheets (~7 nm thickness, denoted as NS-CuO@SAPO-34 in the context) shows an excellent catalytic performance for one-pot oxidation of cyclohexane to adipic acid using O_2 as oxidant (conversion: 42%; selectivity: 74%), which should be the top results of heterogeneous catalysis reported in the literature up to

[a] Dr. X.K. Guo, Ms. M.X. Xu, Mr. M.Y. She, Dr. T.T. Shi, Prof. Y. Zhu, Prof. Z.X. Chen, Prof. L.M. Peng, Prof. X.F. Guo, Prof. W.P. Ding
School of Chemistry and Chemical Engineering
Nanjing University
Nanjing 210023, China
E-mail: guoxf@nju.edu.cn, dingwp@nju.edu.cn
[b] Dr. M. Li
Institute of Materials Research and Engineering
Agency for Science, Technology and Research (A*STAR)
3 Research Link, Singapore 117602, Singapore

Supporting information including experimental details and Figures S1~S16 are given via a link at the end of the document.

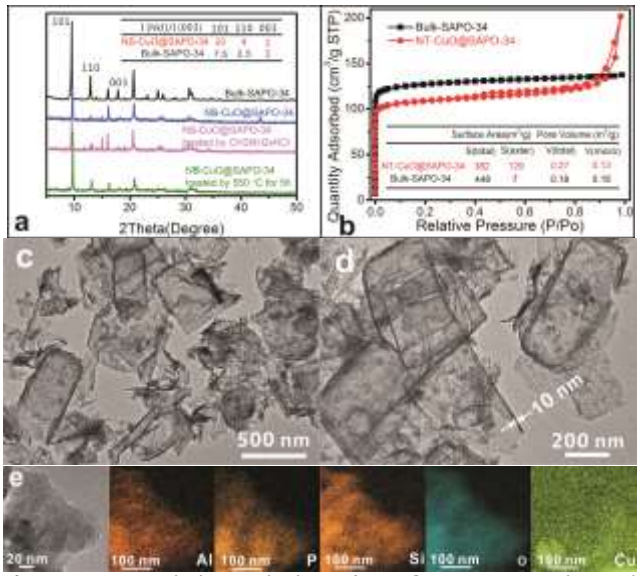

Figure 2. Structural characterizations of CuO@SAPO-34 nanosheets: (a) XRD patterns and (b) Ar sorption/desorption isotherms of NS-CuO@SAPO-34 and bulk-SAPO-34; (c) and (d) TEM images; (e) Elements mapping of the NS-CuO@SAPO-34.

date for the reaction. The adipic acid is one of the most important industrial chemicals for the production of nylon-66 polymer and now, it is produced almost using the non-green method of nitric acid oxidation with very low overall product yields (<10%) and severe environment problems, such as corrosion and emission of vast amount of NOx.[7] In the past decades, great efforts have been devoted to green methods for production of adipic acid and the most recent significant progress is reported by Hwang *et al*, using ozone as oxidant under irradiation of UV light.[6b] However, the direct oxidation of cyclohexane using O_2 via a heterogeneous process to adipic acid remains a great challenge at the present time.[7a] Hence, we envision that the new concept of pore mouth catalysis will be dedicated to open a new spectrum of high-performance catalysts for such difficult reactions.

Figure 1 schematically illustrates the fabrication process of CuO@SAPO-34 nanosheets. Firstly, artificial $AlPO_4$ nanorolls, with nanosheets rolled up, were synthesized according our previous work with dodecylamine bilayers in the $AlPO_4$ nanosheet (SI, TEM image shown as Figure S1).[8] Then tetraethylorthosilicate (TEOS) and $Cu(NO_3)_2$ were introduced into the interlayers of the AlPO4 nanoroll, which were exfoliated under the synthetic conditions, as revealed by XRD measurements (SI, Figure S2). Finally, the nanosheets with CHA crystal structure formed by hydrothermal treatment of the above composite from $AlPO_4$ nanorolls with co-existence of tetraethylammonium hydroxide (TEAOH) and triethylamine (TEA). During the synthesis, the dodecylamine bilayers played a pivotal role, i.e., ensuring a template-confining structure offered for the reaction of ultrathin layer of $AlPO_4$ with TEOS and $Cu(NO_3)_2$ to NS-CuO@SAPO-34.

The organic templates in the as-synthesized product, about 40 wt.% as analyzed by thermogravimetric measurement (SI, Figure S3), can be completely removed by extraction with a methylamine hydrochloride/ethanol solution followed by

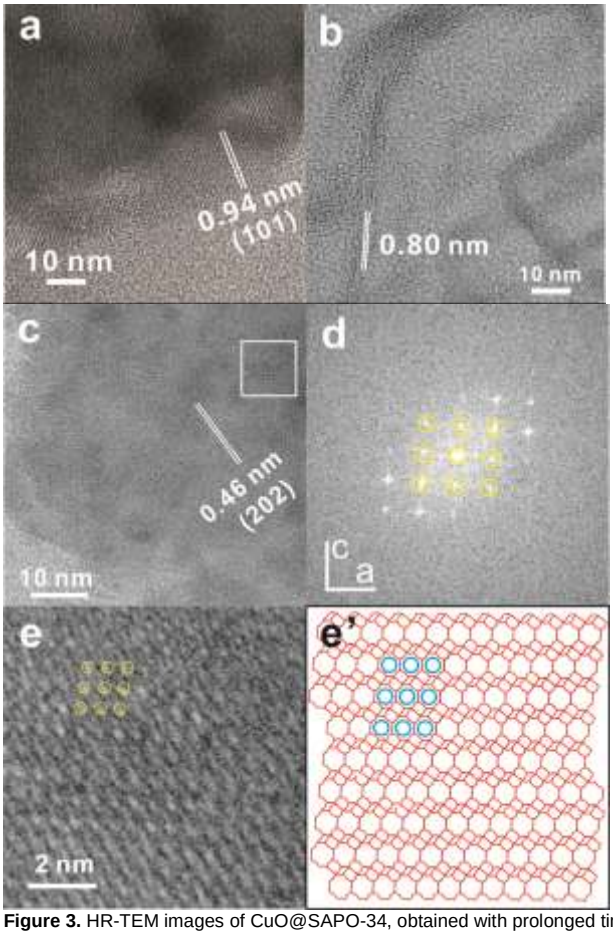

Figure 3. HR-TEM images of CuO@SAPO-34, obtained with prolonged time of exposure to very low current (5 electrons/nm2/sec) at 60 kV. (a), (b) and (c) HRTEM images and (d) SAED pattern of a CuO@SAPO-34 nanosheets (NS-CuO@SAPO-34). (e) HRTEM image of the micro-porous structure enlarged from the white square part in (c). (e') Crystal model corresponding to the TEM image of (e).

calcination at 550 °C in air. The XRD patterns of the related samples obtained during the treatments are shown in Figure 2a. All the peaks are well indexed to CHA type (SAPO-34) without any observable peaks from a secondary phase other than SAPO-34. Moreover, the (101) diffraction peak of the nanosheets exhibits a markedly enhanced intensity (inset, Fig. 2a) than that of the bulk SAPO-34, suggesting the thickness direction of the nanosheets is along the *b* axis of the molecular sieves.[4b] The Ar sorption isotherms of NS-CuO@SAPO-34 have an uptake step below P/P_0=0.02 due to its rich micropores similar to bulk SAPO-34 and a hysteresis loop at P/P_0=0.8~1 indicates the presence of interconnected pores formed by the aggregation of nanosheets (Figure 2b).[9] Compared with bulk SAPO-34, NS-CuO@SAPO-34 has a little smaller Density Functional Theory (DFT) area (382 vs. 448 m^2/g), but a much larger external surface area (129 m^2/g, ~18 times larger than bulk SAPO-34). By calculation, the external surface area of NS-CuO@SAPO-34 corresponds to the nanosheets inaverage thickness of ~7 nm, which closes to theoretical external surface area (147 m^2/g) in such thickness. N_2 sorption/desorption isotherms also show the similar results, as show in Figure S4 (SI).

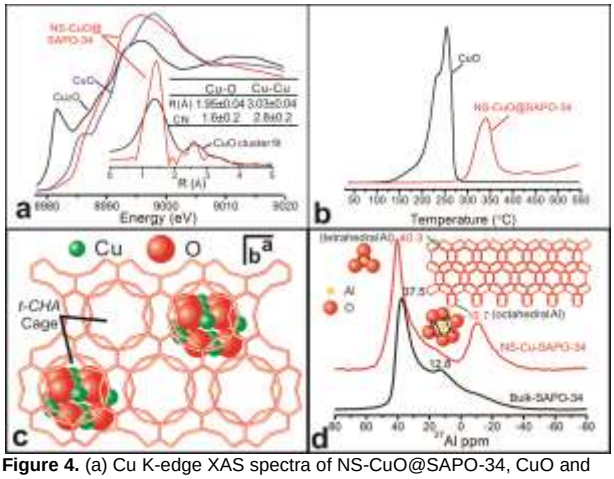

Figure 4. (a) Cu K-edge XAS spectra of NS-CuO@SAPO-34, CuO and Cu_2O. Inset is radial function of Cu from Fourier transform of EXAFS of the NS-CuO@SAPO-34 (the fitting curve is a CuO cluster with the size of 0.7 nm and the table of inset lists the parameters about the copper coordination status); (b) H_2-TPR curves of NS-CuO@SAPO-34 and CuO; (c) Structural model for the skeleton of NS-CuO@SAPO-34; (d) ^{27}Al solid state NMR spectra of NS-CuO@SAPO-34.

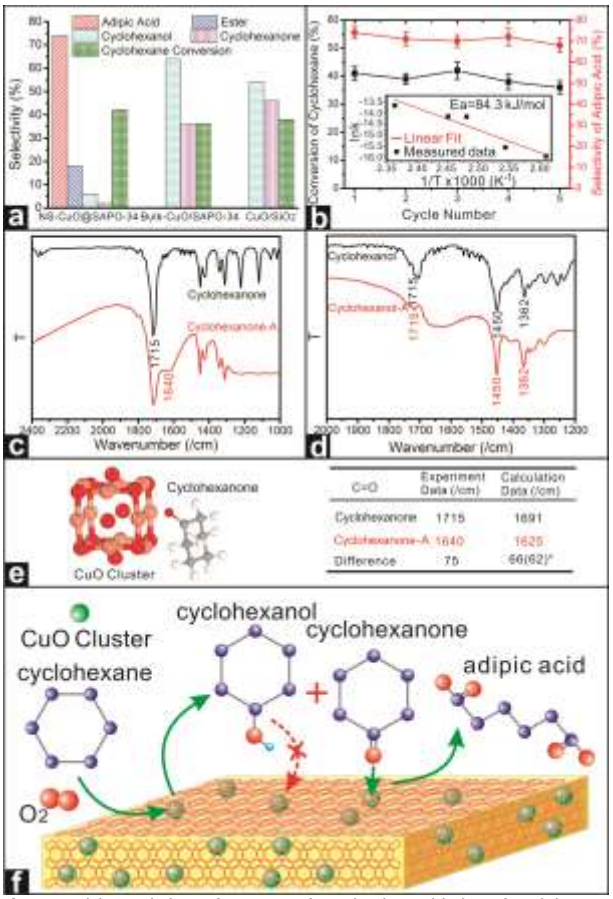

Figure 5. (a) Catalytic performances for selective oxidation of cyclohexane to adipic acid measured with NS-CuO@SAPO-34, bulk-CuO/SAPO-34 and CuO/SiO_2 used as the catalyst. (b) Reusability of the NS-CuO@SAPO-34 for the reaction (Error bars represent the standard deviation for three replicates), and the inset is the Arrhenius' relation of the reaction. In-situ IR spectra of cyclohexanone (c) and cyclohexanol (d) adsorbed on NS-CuO@SAPO-34. (e) The calculation model and results for the IR data, and the number in the brackets is corrected by a coefficient of 0.95 (the results were calculated using DFT method with Gaussian software). (f) Schematic show of catalytic mechanism over NS-CuO@SAPO-34.

The TEM images (Figures 2c and 2d) and SEM images (SI, Figure S5) show the nanosheets are thin rectangles in the sizes of 200-500 nm. As shown in Figure 2e, the elements mapping of NS-CuO@SAPO-34 shows the elements of Al, P, Si and O are all uniform distributed throughout the sample and the domains with Cu enrichment are not detected for their too small sizes. As seen in Figure 3a, the HR-TEM image reveals the nanosheet has a single crystalline structure with a lattice fringe of 0.94 nm, corresponding to the (101) planes of SAPO-34 as the structural model (SI, Figure S6a). Figure 3b showing the cross-section at the curl of a nanosheet reveals its thickness of ~7 nm with a *d*-spacing of 0.80 nm, corresponding to the (0, 3/2, 0) planes of SAPO-34, as the structural model listed in Figure S6b. The thickness of ~7 nm corresponds to ~5 unit cells along the *b*-axis (*b* = 1.3675 nm). Another HRTEM image (Figure 3c) has provided a further proof that the nanosheet has a single crystalline structure with a lattice fringe of 0.46 nm, corresponding to the (202) planes of SAPO-34. The selected area electron diffraction (SAED) (Figure 3d) shows a regular spot pattern when viewed along the *b* axis, which further confirms the single crystalline structure of SAPO-34 nanosheet. Figure 3e shows HRTEM image of the micropore structure of the nanosheet, referred to the corresponding crystal model shown as Figure 3e'. And more HRTEM images (SI, Figure S7) give similar results that the thickness direction of the nanosheet is along the (010) direction of the CHA framework, implying the plane of the nanosheets with many pores is the (010) surface of the SAPO-34.

Electron paramagnetic resonance (EPR) identifies the existence of Cu^{2+} species with axisymmetric octahedrally coordinated status in the cages of CHA (SI, Figure S8).[10] And the X-ray absorption near-edge structure (XANES) spectrum (Figure 4a) indicates the similarity of copper in NS-CuO@SAPO-34 to CuO.[11] By fitting the Cu radial function, the average coordination number of Cu-Cu shell, the most important parameter about the CuO clusters, is found about 2.8±0.2, implying the size of the CuO clusters is ~ 0.7 nm, in accordance to the position they located. In addition, as revealed by the results of hydrogen temperature programmed reduction (H_2-TPR), the NS-CuO@SAPO-34 present a single reduction peak at 340 °C, much higher than that for the reduction by hydrogen of the CuO itself, showing the strong interaction of stabilization of CuO clusters by the molecular sieves enclosing (Figure 4b).[12] Summarizing these results, a structure model of NS-CuO@SAPO-34 is proposed and depicted in Figure 4c and Figure S9 (SI), i.e., CuO clusters (~0.7 nm) with 14 atoms (8 Cu and 6 O) occupied some cages (*t-CHA*) of the SAPO-34 and coordinated the oxygen atoms in framework of *t-CHA* cages. Moreover, the size of CuO clusters is confined by the space of the *t-CHA* cages.

The solid-state ^{27}Al NMR spectrum of the nanosheets (Figure 4d) shows a strong peak at 40.3 ppm belonged to tetrahedral Al similar to bulk SAPO-34.[13a] Interestingly, another peak is observed at -10.7 ppm appeared to be octahedral Al species which cannot be observed, or very little, on bulk SAPO-34. According to the unique morphology of the sample NS-CuO@SAPO-34, the peak is tentatively attributed to the large amount of open cages at the (010) surface of the nanosheet,

consulting with the results of HRTEM and XRD. For ^{31}P NMR spectra (SI, Figure S10), both the samples NS-CuO@SAPO-34 and bulk SAPO-34 show similar ^{31}P-NMR spectra and the main peak at -26 ppm which indicates the tetrahedral P species. [13b] The shoulder peak at -15 ppm is more likely from hydroxylated phosphate. The results imply that the NS-CuO@SAPO-34 has a relative enrichment of aluminum on the top surface, most likely on the top (010) surfaces of the nanosheets.

Figure 5a shows the catalytic results of the NS-CuO@SAPO-34 for oxidation of cyclohexane to adipic acid by O_2 and the results obtained on Bulk-CuO/SAPO-34 and CuO/SiO_2 are also listed for comparison. The reaction data are obtained by analysis performed on isolated products and the adipic acid has been identified by NMR measurements (SI, Figure S11). Excitingly, the selectivity to adipic acid measured on isolated products reaches ~74% at the cyclohexane conversion as high as ~42% are obtained on NS-CuO@SAPO-34 which should be the top results of heterogeneous catalysis reported in the literature up to date (SI, Figure S12) and besides adipic acid, some dicyclohexyl adipate are found as by-product in 20-hour reaction. In sharp contrast, almost no adipic acid products are detected over the samples of Bulk-CuO/SAPO-34 or CuO/SiO_2 as catalyst and only small amount of cyclohexanol and cyclohexanone were detected in the products. We think that the CuO is the reactive center for the catalytic reaction, for the SAPO-34 itself is inactive for the reaction. After the reaction, the leached copper species from the catalyst cannot be detected in the solution using ICP-MS, reflecting the stability of the catalyst. Moreover, the NS-CuO@SAPO-34 shows no obvious degeneration in catalytic performance during the 5 times of reuses in duration of 100 hours (Figure 5b).[14] As shown in inset of Figure 5b and Figure S13 (SI), we also studied the catalytic kinetics and found the apparent activation energy is ~84.3 kJ/mol and reaction order of cyclohexane is ~ 1.5 for the selective oxidation of cyclohexane.

For insight into the mechanism of reaction, cyclohexanol, cyclohexanone or adipic acid, instead of cyclohexane, was respectively used as the reactant (SI, Figure S14). It was discovered that the selectivity to adipic acid reaches ~60% at conversion of 34% when cyclohexanone was used as reactant. Interestingly, no any meaningful products were detected when cyclohexanol or adipic acid was used as the reactant. For adsorptions of cyclohexane, cyclohexanone or cyclohexanol by the NS-CuO@SAPO-34 (SI, Figure S15), it is interesting that the NS-CuO@SAPO-34 catalyst prefers to adsorb cyclohexanone, compared with cyclohexanol, and the adsorption amount of cyclohexanone is about 50% higher than cyclohexanol (0.15 mmol/g vs 0.10 mmol/g). The amount of CuO clusters enclosed in the cages of the sub-surface is 0.17 mmol/g, which is similar to the adsorption amount of cyclohexanone. Based on these results, we think that cyclohexanone tends to adsorb at the CuO clusters through the pores while cyclohexanol tends to adsorb at the pores without CuO clusters. FT-IR spectra recorded with the cyclohexanone or cyclohexanol adsorbed samples have confirmed the conclusion (Figure 5c and 5d). For cyclohexanone adsorption, the newly appeared peak at 1640 cm^{-1} is ascribed to the C=O bond of cyclohexanone chemically adsorbed on the CuO cluster which is shifted from 1715 cm^{-1}, as proved by DFT calculations using Gaussian software and B3LYP method (Figure 5e), which reflects the strong interaction between the C=O group of cyclohexanone and CuO clusters in the NS-CuO@SAPO-34. For cyclohexanol, however, no chemical adsorption can be found by the FT-IR spectrum, which is the same with liquid cyclohexanol (Figure 5d). Hence, it is proposed that cyclohexane firstly converts to cyclohexanone as the main intermediate with minor cyclohexanol as by product, as shown in Figure 5f. Secondly, the cyclohexanone molecules are chemically adsorbed on the partially confined CuO cluster sites and start to be oxidized to adipic acid in the following catalytic reactions.[7e] The high selectivity of adipic acid should be attributed to the strong confining effect of the channel mouths on the interactions between the reactant and CuO clusters which are the reactive centers under the top surface of the NS-CuO@SAPO-34. To understand the activation of O_2, the coordinated environment of CuO clusters and free radicals of oxygen species were detected by EPR, as shown in Figure S16 (SI). We believe it may not be a radical mechanism but a mechanism that the CuO clusters oxidized cyclohexane molecular by their lattice oxygen and O_2 re-oxidize the CuO clusters and the turnover frequency of cyclohexane conversion is 29.4 h^{-1} per cluster.

In summary, a new kind of hybrid material, CuO@SAPO-34 nanosheet is prepared via a newly demonstrated mechanism of exfoliation and crystallization of layered $AlPO_4$ precursor with morphology reserved. The CuO@SAPO-34 nanosheet has exhibited high crystallinity, large external surface and excellent hydrothermal stability. It shows an excellent catalytic performance for the selective oxidation of cyclohexane to adipic acid using molecular oxygen as oxidant, which holds the potential as a practical catalyst to produce adipic acid in an efficient and green way. And also, we envision that the new concept of pore mouth catalysis extracted from the current investigation will be dedicated to open a new spectrum of design for high-performance catalysts.

Experimental Section

Experimental Details and Figures S1~S16 see supporting information.

Acknowledgements

This work was financially supported by National Science Foundation of China (21773110, 21773109, 21932004 and 91745108), the Ministry of Science and Technology of China (2017YFB0702900) and the Fundamental Research Funds for the Central Universities and Jiangsu Overseas Visiting Scholar Program for University Prominent Young & Middle-aged Teachers and Presidents. We thank the help from Mr. Jason Gulbinski and Dr. Wei Fan in UMass Amherst for their proof reading on the manuscript.

Keywords: molecular sieves • oxide cluster • nanosheet • pore mouth catalysis • selective oxidation

[1] a) F. R. Fortea-Pérez, M. Mon, J. Ferrando-Soria, M. Boronat, A. Leyva-Pérez, A. Corma, J. M. Herrera, D. Osadchii, J. Gascon, D.

Armentano, E. Pardo, *Nat. Mater.* **2017**, *16*, 760-766; b) L. Wang, G. X. Wang, J. Zhang, C. Q. Bian, X. J. Meng, F. S. Xiao, *Nat. Commun.* **2017**, *8*, 15240 doi: DOI: 10.1038/ncomms15240; c) L. C. Liu, U. Díaz, R. Arenal, G. Agostini, P. Concepción, A. Corma, *Nat. Mater.* **2017**, *16*, 132-138; d) N. Wang, Q. M. Sun, R. S. Bai, X. Li, G. Q. Guo, J. H. Yu, *J. Am. Chem. Soc.* **2016**, *138*, 7484-7487.

[2] a) O. Fenwick, E. Coutiño-Gonzalez, D. Grandjean, W. Baekelant, F. Richard, S. Bonacchi, D. D. Vos, P. Lievens, M. Roeaers, J. Hofkens, P. Samorì, *Nat. Mater.* **2016**, *15*, 1017-1022; b) S. Goel, Z. Wu, S. I. Zones, E. Iglesia, *J. Am. Chem. Soc.* **2012**, *134*, 17688-17695; c) N. Kosinov, C. Liu, E. J. M. Hensen, E. A. Pidko, *Chem. Mater.* **2018**, *30*, 3177-3198; d) J. B. Han, J. Cho, J. C. Kim, R. Ryoo, *ACS Catal.* **2018**, *8*, 876-879.

[3] a) D. Dubbeldam, S. Calero, T. L. M. Maesen, B. Smit, *Angew. Chem. Int. Ed.* **2003**, *42*, 3624-3626; b) M. Dusselier, M. E. Davis, *Chem. Rev.* **2018**, *118*, 5265-5329.

[4] a) W. J. Roth, P. Nachtigall, R. E. Morris, J. Čejka, *Chem. Rev.* **2014**, *114*, 4807-4837; b) M. Choi, K. Na, J. Kim, Y. Sakamoto, O. Terasaki, R. Ryoo, *Nature* **2009**, *461*, 246-249; c) L. M. Ren, Q. Guo, P. Kumar, M. Orazov, D. D. Xu, S. M. Alhassan, K. A. Mkhoyan, M. E. Davis, M. Tsapatsis, *Angew. Chem. Int. Ed.* **2015**, *54*, 10848-10851; d) F. Lin, J. Y. Zhang, D. X. Liu, Y. H. Chin, *Angew. Chem. Int. Ed.* **2018**, *57*, 12886 -12890.

[5] a) F. Solanea, O. Ramos, M. K. de Pietre, H. O. Pastore, *RSC Adv.* **2013**, *3*, 2084-2111; b) M. V. Opanasenko, W. J. Rothab, J. Čejka, *Catal. Sci. Technol.* **2016**, *6*, 2467-2484; c) J. Prech, P. Pizarro, D. P. Serrano, J. Cejka, *Chem. Soc. Rev.* **2018**, *47*, 8263-8306; d) P. Eliasova, M. Opanasenko, P. S. Wheatley, M. Shamzhy, M. Mazur, P. Nachtigall, W. J. Roth, R. E. Morris, J. Cejka, *Chem. Soc. Rev.* **2015**, *44*, 7177-7206.

[6] M. Y. Jeon, D. Kim, P. Kumar, P. S. Lee, N. Rangnekar, P. Bai, M. Shete, B. Elyassi, H. S. Lee, K. Narasimharao, S. N. Basahel, S. Al-Thabaiti, W. Xu, H. J. Cho, E. O. Fetisov, R. Thyagarajan, R. F. DeJaco, W. Fan, K. A. Mkhoyan, J. I. Siepmann, M. Tsapatsis, *Nature* **2017**, *543*, 690-694.

[7] a) M. Dugal, G. Sankar, R. Raja, J. M. Thomas, *Angew. Chem. Int. Ed.* **2000**, *39*, 2310-2313; b) K. C. Hwang, A. Sagadevan, *Science* **2014**, 346, 1495-1498; c) K. Sato, M. Aoki, R. Noyori, *Science* **1998**, *281*, 1646-1647; d) T. Iwahama, K. Syojyo, S. Sakaguchi, Y. Ishii, *Organic Process Research & Development* **1998**, *2*, 255-260; e) S. A. Chavan, D. Srinivas, P. Ratnasamy, *Journal of Catalysis* **2002**, *212*, 39-45; f) D. Bonnet, T. Ireland, E. Fachea, J. P. Simonato, *Green Chem.* **2006**, *8*, 556-559; g) S. V. Vyver, Y. Roman-Leshkov, *Catal. Sci. Technol.* **2013**, *3*, 1465-1479.

[8] X. K. Guo, Q. L. Ma, X. F. Guo, W. P. Ding, Y. Chen, *Chem. Commun.* **2009**, 3443-3445.

[9] D. D. Xu, Y. H. Ma, Z. F. Han, L. Jing, B. Singh, J. Feng, X. F. Shen, F. L. Cao, P. Oleynikov, H. Sun, O. Terasaki, S. A. Che, *Nat. Commun.* **2014**, *5*, 4262 doi: 10.1038/ncomms5262.

[10] a) K. Narsimhan, V. K. Michaelis, G. Mathies, W. R. Gunther, R. G. Griffin, Y. Román-Leshkov, *J. Am. Chem. Soc.* **2015**, *137*, 1825-1832; b) T. N. Ryu, H. Ahn, S. Seo, J. Cho, H. Kim, D. Jo, G. T. Park, P. S. Kim, C. H. Kim, E. L. Bruce, P. A. Wright, I. S. Nam, S. B. Hong, *Angew. Chem. Int. Ed.* **2017**, *56*, 3256-3260.

[11] a) C. W. Andersen, E. Borfecchia, M. Bremholm, M. R. V. Jørgensen, P. N. R. Vennestrøm, C. Lamberti, L. F. Lundegaard, B. B. Iversen, *Angew. Chem. Int. Ed.* **2017**, *56*, 10367-10372; b) A. Martini, E. Borfecchia, K. A. Lomachenko, I. A. Pankin, C. Negri, G. Berlier, P. Beato, H. Falsig, S. Bordiga, C. Lamberti, *Chem. Sci.* **2017**, *8*, 6836-6851.

[12] D. Wang, L. Zhang, J. H. Li, K. Kamasamudram, W. S. Epling, *Catalysis Today* **2014**, *231*, 64-74.

[13] a) D. Fan, P. Tian, S. T. Xu, Q. H. Xia, X. Su, L. Zhang, Y. Zhang, Y. L. He, Z. M. Liu, *J. Mater. Chem.* **2012**, *22*, 6568-6574; b) K. Shen, W. Z. Qian, N. Wang, C. Su, F. Wei, *J. Am. Chem. Soc.* **2013**, *135*, 15322-15325.

[14] G. Y. Yang, Y. X. Wei, S. T. Xu, J. R. Chen, J. Z. Li, Z. M. Liu, J. H. Yu, R. R. Xu, *J. Phys. Chem. C* **2013**, *117*, 8214-8222.

10.1002/anie.201911749

WILEY-VCH

COMMUNICATION

2D and super-thin CuO@SAPO-4 nanosheets with ~7 nm thickness and single crystalline structure have been synthesized and shown an excellent catalytic performance for the selective oxidation of cyclohexane to adipic acid using molecular oxygen as oxidant by a pore mouth catalysis mechanism.

X. Guo, M. Xu, M. She, Y. Zhu, T. Shi, Z. Chen, L. Peng, X. Guo, M. Lin,* W. Ding**

Page No. – Page No.

Morphology Reserved Synthesis of Discrete Nanosheets of CuO@SAPO-34 and Pore Mouth Catalysis for One-pot Oxidation of Cyclohexane